

Molecules in the $z_{\text{abs}} = 2.8112$ damped system toward PKS 0528–250*

R. Srianand¹ and Patrick Petitjean^{2,3}

¹IUCAA, Post Bag 4, Ganesh Khind, Pune 411 007, India

²Institut d’Astrophysique de Paris – CNRS, 98bis Boulevard Arago, F-75014 Paris, France

³UA CNRS 173 – DAEC, Observatoire de Paris-Meudon, F-92195 Meudon Cedex, France

Abstract. We present a detailed analysis of a high resolution spectrum of the damped Ly α system at $z_{\text{abs}} = 2.8112$ toward PKS 0528-250. The absorption redshift is slightly larger than the emission redshift of the quasar. We estimate the column density of H₂ molecules $N(\text{H}_2) \sim 6 \times 10^{16} \text{ cm}^{-2}$ and the fractional abundance of H₂, $f = 5.4 \times 10^{-5}$. The excitation temperature derived for different transitions suggests that the kinetic temperature of the cloud is ~ 200 K and the density $n \sim 1000 \text{ cm}^{-3}$. The cloud therefore has a dimension of ~ 1 pc along the line of sight. Since it obscures the broad-line emission region, its transverse dimension should be larger than 10 pc.

We obtain upper limits on the column densities of C I ($< 10^{12.7} \text{ cm}^{-2}$) and CO ($< 10^{13.2} \text{ cm}^{-2}$; $N(\text{CO})/N(\text{H I}) < 7 \times 10^{-9}$). We suggest that the ratio $N(\text{H}_2)/N(\text{C I})$ is a useful indicator of the physical conditions in the absorber. Simple photo-ionization models assuming solar relative abundances show that radiation fields with spectra similar to typical AGNs or starbursts are unable to reproduce all the constraints and in particular the surprisingly small $N(\text{C I})/N(\text{H}_2)$ and $N(\text{Mg I})/N(\text{H}_2)$ ratios. In view of the models we explored, the most likely ionizing spectrum is a composite of a UV-“big bump” possibly produced by a local starburst and a power-law spectrum from the QSO that provides the X-rays. Dust is needed to explain the production of molecules in the cloud. The amount of dust is broadly consistent with the [Cr/Zn] abundance determination.

Key words: Galaxies: ISM, quasars:absorption lines, quasars:individual:PKS 0528–250, Galaxies: halo

1. Introduction

QSO absorption line systems probe the baryonic matter over most of the history of the Universe ($0 < z \lesssim 5$). The so-called damped Ly α (hereafter DLA) systems are characterized by a very large H I column density ($N(\text{H I}) \gtrsim 2 \times 10^{20} \text{ cm}^{-2}$), similar to the one usually seen through local spiral disks. The case for these systems to be produced by proto-galactic disks is supported by the fact that the cosmological density of gas associated with these systems is of the same order of magnitude as the cosmological density of stars at present epochs (Wolfe 1996). Moreover the presence of heavy elements ($Z \sim 0.1 Z_{\odot}$) and the redshift evolution of metallicity suggest the ongoing star formation activities in these systems (Pettini et al. 1997), while strong metal line systems have been demonstrated to be associated with galaxies at low and intermediate z (e.g. Bergeron & Boissé 1991). It has also been shown that the profiles of the lines arising in the neutral gas show evidence for rotation (Wolfe 1996, Prochaska & Wolfe 1997). Whether these arguments are enough to demonstrate that DLA systems arise in large disks is a matter of debate however. Indeed simulations have shown that the progenitors of present day disks of galaxies could look like an aggregate of well separated dense clumps at high redshift. The kinematics could be explained by relative motions of the clumps with very little rotation (Haehnelt et al. 1997, Ledoux et al. 1998). Moreover, using *HST* high spatial resolution images of the field of seven quasars whose spectra contain DLA lines at intermediate redshifts ($0.4 \lesssim z \lesssim 1$), Le Brun et al. (1996) show that, in all cases, at least one galaxy candidate is present within 4 arcsec from the quasar. There is no dominant morphological type in their sample: three candidates are spiral galaxies, three are compact objects and two are amorphous low surface brightness galaxies. Therefore, although the nature of the DLA systems is unclear they trace the densest regions of the Universe where star formation occurs.

Send offprint requests to: R. Srianand

* Based on observations collected at the European Southern Observatory, La Silla, Chile

It is thus surprising that despite intensive searches, the amount of H_2 molecules seems quite low in DLA systems in contrast to what is observed in our own galaxy. Two detections of H_2 molecules in high redshift DLA systems have been reported. Recently Ge & Bechtold (1997) have found strong absorptions in the $z_{\text{abs}} = 1.9731$ DLA system toward Q 0013–004. They derive $N(\text{H}_2) = 6.9 \times 10^{19} \text{ cm}^{-2}$, $b = 15 \text{ km s}^{-1}$, $T_{\text{ex}} \sim 70 \text{ K}$ and $n(\text{H}) \sim 300 \text{ cm}^{-3}$ for a total hydrogen column density $N(\text{H}) = 6.4 \times 10^{20} \text{ cm}^{-2}$. This system has by far the largest H_2 abundance $f = 2N(\text{H}_2)/[2N(\text{H}_2) + N(\text{H I})] \sim 0.22 \pm 0.05$ observed in high z DLA systems. However the exact number should be confirmed using a higher resolution data. Other searches have led to much smaller values or upper limits ($f < 10^{-6}$, Black et al. 1987, Chaffee et al. 1988, Levshakov et al. 1992). Levshakov & Varsshalovich (1985) suggested that H_2 molecules could be present in the $z_{\text{abs}} = 2.8112$ system toward PKS 0528–250. This claim has been confirmed by Foltz et al. (1988) using a 1 \AA resolution spectrum. The latter authors derive $N(\text{H}_2) = 10^{18} \text{ cm}^{-2}$, $b = 5 \text{ km s}^{-1}$, $T_{\text{ex}} = 100 \text{ K}$ and $\log N(\text{H I}) = 21.1 \pm 0.3$. By fitting the damped absorption together with the $\text{Ly}\alpha$ emission from the quasar, Møller & Warren (1993) find $\log N(\text{H I}) = 21.35$. Three $\text{Ly}\alpha$ emission-line objects have been detected within $100h^{-1} \text{ kpc}$ from the quasar by Møller & Warren (1993) and confirmed by Warren & Møller (1996) to have redshifts within 200 km s^{-1} from the redshift of the DLA system ($z_{\text{abs}} = 2.8112$ as measured on the Ni II lines by Meyer & York 1987). The widths of the $\text{Ly}\alpha$ emission lines are very large ($> 600 \text{ km s}^{-1}$) and continuum emission could be present (Warren & Møller 1996); this suggests that the gas is not predominantly ionized by the quasar and that star-formation may occur in the clouds, a conclusion reached as well by Ge et al. (1997). The proximity of the quasar makes the case difficult however and careful analysis is needed.

In this paper we use much higher spectral resolution data to reanalyze the molecular lines in this system. We present the observations in Section 2, the results in Section 3 and discuss the low $N(\text{C I})/N(\text{H}_2)$ ratio inferred in Section 4.

2. Observations

The observations were carried out at the F/8 Cassegrain focus of the 3.6 m telescope at La Silla, ESO Chile. The spectra were obtained with the ESO echelle spectrograph (CASPEC) and long camera. Three exposures of 5400 s each were obtained under good seeing conditions in November 1995. A 300 line mm^{-1} cross disperser was used in combination with a $31.6 \text{ line mm}^{-1}$ echelle grating. The detector was a Tektronix CCD with 1124×1024 pixels of $15 \mu\text{m}$ square and a read-out noise of 2.5 electrons. For each exposure on the object, flat field images and wavelength comparison Thorium–Argon spectra were

recorded. The slit width was 1.6 arcsec corresponding to a spectral resolution of $R \sim 36000$ over the wavelength range $3650 - 4850 \text{ \AA}$. The spectra were binned in the direction perpendicular to the dispersion axis. The accuracy in the wavelength calibration measured on the calibrated Thorium–Argon spectra is about 0.03 \AA .

The data were reduced using the echelle reduction package provided by IRAF. The cosmic-ray events have been removed in the regions between object spectra before extraction of the object. The exposures were co-added to increase the signal to noise ratio. During this merging procedure the cosmic-ray events affecting the object pixels were recognized and eliminated. The background sky spectrum was difficult to extract separately due to the small spacing between the orders in the blue. Instead, we have carefully fitted the zero level to the bottom of the numerous saturated lines in the $\text{Ly}\alpha$ forest. The uncertainty on the determination can be estimated to be 5%.

We identify all the absorption features with equivalent widths larger than $5 \times \text{FWHM} \times \sigma$ where σ is the noise rms in the adjacent continuum. We use the line list to identify the metal line systems in the spectra and more specifically all the absorptions associated with the $z_{\text{abs}} = 2.8112$ DLA system.

3. Results

3.1. Low ionization metal lines

Table 1. Heavy element lines from the damped system

ION	log N	[Z/H]	Ref
H I	21.35 ± 0.10	...	1
C I	< 12.77	...	3
Ar I	14.46 ± 0.23	-1.43 ± 0.63	3
Mg I	< 12.8		2,3
Mg II	< 15.88	< -1.04	2
Si II	16.00 ± 0.04	-0.90 ± 0.11	2
S II	15.27 ± 0.06	-1.03 ± 0.04	2
Cr II	13.65 ± 0.12	-1.38 ± 0.16	2
Fe II	15.46 ± 0.09	-1.41 ± 0.05	3
Ni II	13.89 ± 0.03	-1.71 ± 0.10	2
Zn II	13.09 ± 0.07	-0.91 ± 0.12	2

¹ Møller & Warren 1993; ² Lu et al. 1996; ³ This work

Lu et al. (1996) have obtained column densities of most of the elements in the DLA system considered here. In addition to the lines identified by Lu et al (1996) we find a possible Ar I doublet from this molecular cloud (see Fig. 1). Since our spectrum extends further into the blue, we could also obtain a better estimate of the Fe II column density using the lines from very weak transitions (e.g. Fe II $\lambda 1125$, Fe II $\lambda 1127$, Fe II $\lambda 1142$ etc., see Fig. 1). We also obtained an upper limit to the C I column density which will be useful for constraining the model parameters. The column

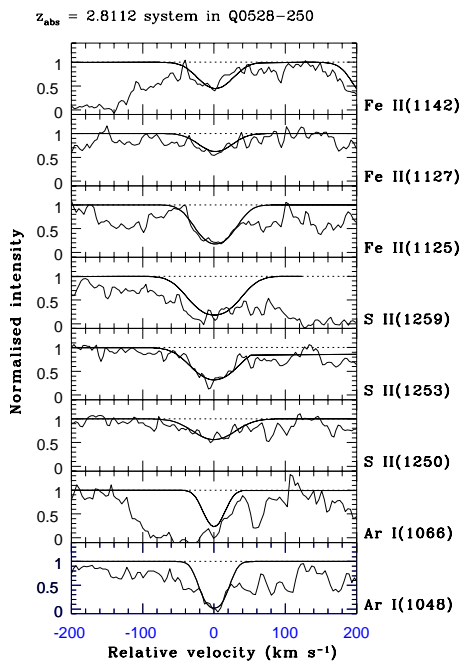


Fig. 1. Fit result for few weak heavy element transitions in the $z_{\text{abs}} = 2.8112$ damped system

densities of different species are given in Table 1. Since in the neutral phase of DLA systems the dominant ionization state of the elements listed in Table 1 is either the neutral (for argon) or the singly ionized (for the others) state, we can estimate element abundances. The values we obtain for the S II column density is about a factor of two less than that of Lu et al. The reason is that we detect and fit only the strongest component whereas Lu et al. integrate the apparent optical depth from $v = -80$ to 300 km s^{-1} . For consistency of the discussion, we adopt the value from Lu et al. Subsequently, since singly ionized species can be found well outside the region where hydrogen is neutral, it must be noticed that the values of the ratios $N(X^+)/N(\text{H I})$ are upper limits.

An interesting limit on the Mg I column density can be obtained from the Lu et al. data. Mg I $\lambda 2026$ is blended with Zn II $\lambda 2026$. However from Fig. 9 of Lu et al., we can see that the optical depth of the line is smaller than 0.1. If we consider, as for Zn II and Cr II that the absorption is spread over 40 km s^{-1} we can infer that $w_{\text{r}} < 0.027 \text{ \AA}$. Using the oscillator strength given by Morton(1991), we find $N(\text{Mg I}) < 6.6 \times 10^{12} \text{ cm}^{-2}$.

Formation of H_2 molecules is most efficient in the presence of dust grains (see Section 3.2). In DLA systems the amount of dust is usually estimated from the ratio $N(\text{Zn II})/N(\text{Cr II})$ assuming that, like in the ISM of our galaxy, Zn is not heavily depleted onto dust grains whereas Cr is depleted (Meyer et al. 1989; Pettini et al. 1994, 1997; Lu et al. 1996). Some controversy has arisen

however about the presence of dust in DLA systems. Lu et al. (1996) have argued that nucleosynthesis alone can explain the element abundance ratios observed in DLA systems and that the presence of dust is thus questionable whereas Pettini et al. (1997) have claimed that even though nucleosynthesis history of the gas must play a role, the consistent depletion levels of the refractory elements indicates the presence of dust. We discuss the abundance ratios of Table 1 considering the two possibilities in turn.

It is known that Zn and S are not heavily depleted into dust grains (Sembach & Savage 1996) and should reflect the gas-phase abundances which is thus of the order of $0.1\text{--}0.2 Z_{\odot}$. The average value of $[\text{Cr}/\text{Zn}]$ in the diffuse interstellar clouds with molecular fraction $\log f(\text{H}_2)$ between -6 and -4 is -1.18 ± 0.53 (Roth & Blades 1995). The observed $[\text{Cr}/\text{Zn}] = -0.47$ in the $z = 2.8112$ system suggests that about 70% of Cr is depleted onto dust grains in the damped system compared to 99% in the diffuse interstellar medium of our galaxy. The observed Ni II/Cr II in the 2.8112 system is consistent with the ratio in the interstellar medium. Silicon has the same gas-phase abundance as zinc (see Table 1) which is consistent with the much lower depletion of silicon as compared to iron, chromium and nickel in the interstellar medium. The non detection of Mg I is intriguing. Although the upper limit on Mg II is consistent with the other element abundances, some depletion could be needed (see Section 4). All these are consistent with the presence of dust in the system with small departure of the total element abundance ratios from the solar values.

It is interesting to note however that in our galaxy, stars with $[\text{Fe}/\text{H}] \sim -1$, have $[\text{Si}/\text{Fe}] \sim [\text{S}/\text{Fe}] \sim 0.4$ (e.g. François 1987) and $[\text{Cr}/\text{Fe}] \sim [\text{Ni}/\text{Fe}] \sim 0$ (Magain 1989, Gratton & Sneden 1991) which is approximately what we observe. Thus the assumption of depletion onto dust grains may be questionable. The upper limit on magnesium is consistent with $[\text{Mg}/\text{Fe}] \sim 0.4$ (Magain 1989). However a better limit on this element would definitively be very helpful. However if we accept the gas-phase metallicities as the true metallicities, then the observed value $[\text{Zn}/\text{Fe}] = 0.5$ is not consistent with the value observed in the same stars ($[\text{Zn}/\text{Fe}] = 0$, Sneden & Crocker 1988).

In the case of the $z_{\text{abs}} = 2.8112$ system toward PKS 0528–250, we can investigate further this issue by asking the question whether dust is needed to produce the observed amount of H_2 molecules (see Section 4).

3.2. H_2 molecules

The consequence of the spectral resolution being nine times larger than the previous published data can be appreciated by comparing Fig. 2 with Fig. 4 of Foltz et al. (1988). In our data, a large number of molecular lines are left unblended making the determination of the line parameters much reliable.

We have derived the $N(\text{H}_2)$ and b values using a Voigt profile fitting code (Khare et al. 1997). The oscillator strengths of different transitions given in Morton & Dinerstein (1976) have been used. Only the clean and unblended lines from each rotational level are fitted. The best fit is obtained with a single component model although a few discrepancies between the fit and the data may argue for a two-component model (see also the comment by Jenkins & Peimbert 1997 about this system). The resulting fit is shown in Fig. 2 for a few transitions. The fit parameters are given in Table 2 where the second, third and fourth columns give the statistical weights of different levels, the column density and the number of lines used in the model respectively. The best value for the velocity dispersion is $b = 9.1 \text{ km s}^{-1}$.

Table 2. H_2 column densities and excitation temperatures

LEVEL	g	N_J (10^{16} cm^{-2})	Number	T_{ex} (K)	J_{ex}
$J = 0$	1	0.965 ± 0.330	4
$J = 1$	9	4.110 ± 0.009	7	229 ± 95	0-1
$J = 2$	5	0.417 ± 0.063	8	208 ± 36	0-2
$J = 3$	21	0.216 ± 0.029	3	225 ± 08	0-3
				224 ± 09	1-3
$J = 4$	9	≤ 0.03	...	≤ 300	0-4

The total column density $N(\text{H}_2)$ in the cloud is $6 \times 10^{16} \text{ cm}^{-2}$ and the measured fractional H_2 abundance is $f = 2 N(\text{H}_2) / [2 N(\text{H}_2) + N(\text{H I})] = 5.4 \times 10^{-5}$. This value is obtained using $N(\text{H I}) = 2.2 \times 10^{21} \text{ cm}^{-2}$ (Møller & Warren 1993), and assuming that all the neutral hydrogen contributing to the damped Ly α absorption originates from the same region as H_2 . If this were not the case, f would be higher. The molecular fraction obtained here is two orders of magnitude less than the values quoted by Foltz et al. (1988). However as noted by the latter authors, the column density is very sensitive to the Doppler parameter and their value should be considered as an upper limit.

In the case of thermal equilibrium, the ratio of column densities of two rotational levels are given by the Boltzman equation,

$$\frac{N(J)}{N(0)} = \frac{g_J}{g_0} \exp \left[- \frac{BJ(J+1)}{kT_{\text{ex}}} \right]. \quad (1)$$

where g_J is the statistical weight of any level J in the vibrational ground state, T_{ex} is the excitation temperature and the constant B/k is $\simeq 85 \text{ K}$. The values of T_{ex} derived for different transitions are given in column 5 of Table 2. Lines from higher "J" levels (i.e. $J \geq 4$) are weak and we could derive only upper limits to column densities.

It is believed that the $J = 1$ level is mostly populated by collisions so the excitation temperature, T_{01} , is roughly equal to the kinetic temperature. As can be seen from

Table 2, the excitation temperatures derived for different levels are similar, suggesting that T_{ex} indeed equals the kinetic temperature which is therefore close to $\sim 220 \text{ K}$ in this molecular cloud.

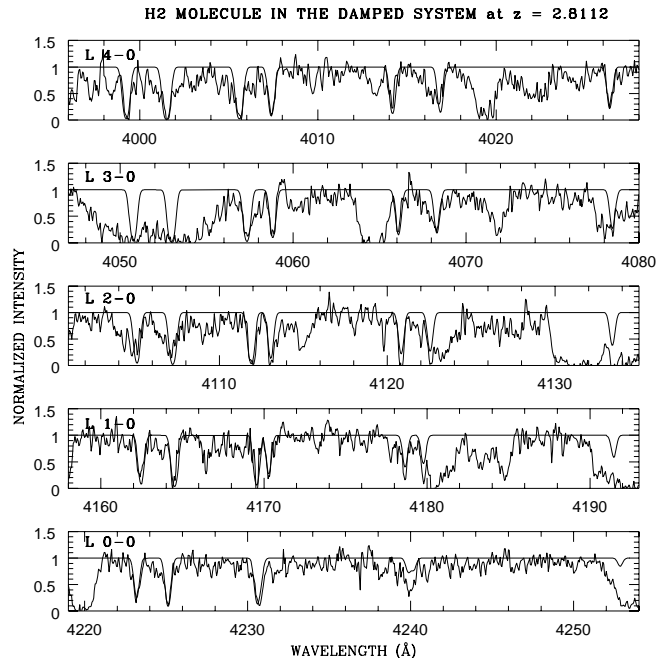


Fig. 2. Fit results for a few rotational transitions of the H_2 Lyman absorption bands in the $z_{\text{abs}} = 2.8112$ damped system

As suggested by Jura (1975) the column density ratio $N(2)/N(0)$ and $N(3)/N(1)$ are controlled by the kinetic temperature when $n(\text{H}) > 20$ and $n(\text{H}) > 300 \text{ cm}^{-3}$ respectively. Our limit on the population of the $J = 4$ rotational level do not add much constraint on the density. However, Ge & Bechtold (1997) report a new determination $N(4)/N(0) = 4.5 \times 10^{-3}$ by Songaila & Cowie (1995). This new value implies an excitation temperature $T_{04} = 224 \text{ K}$. The calculations by Nishimura (1968) indicate that all this is consistent with a kinetic temperature of $T \sim 220 \text{ K}$ and a density $n \sim 1000 \text{ cm}^{-3}$.

Using the asymptotic approximation given by Jura (1974) for the ratio of the molecular to neutral hydrogen densities, $n(\text{H}_2)/n(\text{H})$, as a function of the optical depth within a molecular cloud, we can derive an estimate of the photo-dissociation rate of molecules, I , due to the incident UV flux,

$$I = \frac{nR}{\delta} \sqrt{\frac{N}{2 \langle f \rangle}} \quad (2)$$

where $\delta = 4.2 \times 10^5$, n is the hydrogen density, R is the rate of molecule formation onto dust grains; N is the total

H I column density and $\langle f \rangle$ is the mean molecular fraction observed through the cloud. If we scale R with the metallicities from the value observed in the ISM, then we can estimate that $R \sim 3 \times 10^{-18} \text{ cm}^3 \text{ s}^{-1}$. This may well be an upper limit since the dust to gas ratio in the damped system is smaller than in the ISM (see Section 3.1). Using the density and the molecular fraction derived above (i.e., $n \sim 1000 \text{ cm}^{-3}$ and $f \sim 5.4 \times 10^{-5}$) we estimate the photodissociation rate of molecules, $I \sim 3.2 \times 10^{-8} \text{ s}^{-1}$, and the photo-absorption rate in the Lyman and Werner bands, $\beta_o \sim I/0.11 \sim 3 \times 10^{-7} \text{ s}^{-1}$ (Jura 1975). This large value results from the large H I column density albeit small molecular fraction seen in $z_{\text{abs}} = 2.8112$ damped system. We are confident that f , n and the metallicities are known within a factor of two.

The estimated value of the photo-absorption rate, β_o , is $3 \times 10^{-7} \text{ s}^{-1}$. This value is an order of magnitude higher than the values obtained by Ge & Bechtold (1997). It is also two orders of magnitude higher than the average value for the interstellar radiation field in our galaxy (i.e. $\beta_o = 5 \times 10^{-10} \text{ s}^{-1}$). The average value for the intergalactic medium radiation field calculated for $J_{21}(912 \text{ \AA}) = 1$, is $\beta_o = 2 \times 10^{-12} \text{ s}^{-1}$. Thus the radiation field in the $z = 2.8112$ absorbing cloud is not dominated by the intergalactic UV radiation field. The most probable sources are either the radiation from the quasar or from the young stars in the molecular cloud itself.

If we take quasar alone (see however Section 4) to be the ionizing source then, using $m_B = 18.17$, $q_o = 0.5$, $H_o = 75 \text{ km s}^{-1} \text{ Mpc}^{-1}$, the optical to UV spectral index $\alpha = -1$ ($f_\nu \propto \nu^{-\alpha}$) and the upper limit on β_o , we estimate that the H_2 cloud should be at a distance larger than 10 kpc from the quasar.

If we assume that the H_2 lines are thermally broadened then the velocity dispersion of 9 km s^{-1} gives a kinetic temperature of $\sim 2000 \text{ K}$. This is higher than the kinetic temperature inferred from the excitation temperatures. Thus it is possible that there are more than one component in the H_2 absorption. This may introduce a small error in the total H_2 column density. However the lines are not heavily saturated and hence the errors cannot be large.

3.3. CO molecules

In the galactic diffuse clouds, $N(\text{CO}) \sim 10^{-7} \times N(\text{H})$. As the high redshift DLA systems have, on average, one tenth of the solar metallicity we would expect the $N(\text{CO})/N(\text{H})$ ratio to be lower than 10^{-7} . Indeed optical and radio searches (e.g. Levshakov et al. 1989; Wilkind & Combes 1994 and references therein) fail to detect CO both in emission and absorption in high z damped absorbers.

However CO emission is detected from a few high redshift quasars and ultra-luminous infrared galaxies (see e.g. Barvainis et al. 1994, Ohta et al. 1996; Omont et al. 1996; Guilloteau et al. 1997). These detections suggest that a

large amount of mass in host galaxies (or surrounding regions) of some of the high redshift AGNs is in the form of molecules.

We have searched for the presence of absorption due to CO A-X molecular bands in a $FWHM = 0.6 \text{ \AA}$ spectrum obtained by Petitjean & Bergeron (1994) primarily for studying intervening C IV systems (see their paper for the observational details). No strong CO absorption is detected from the $z = 2.8112$ system (see Fig. 3).

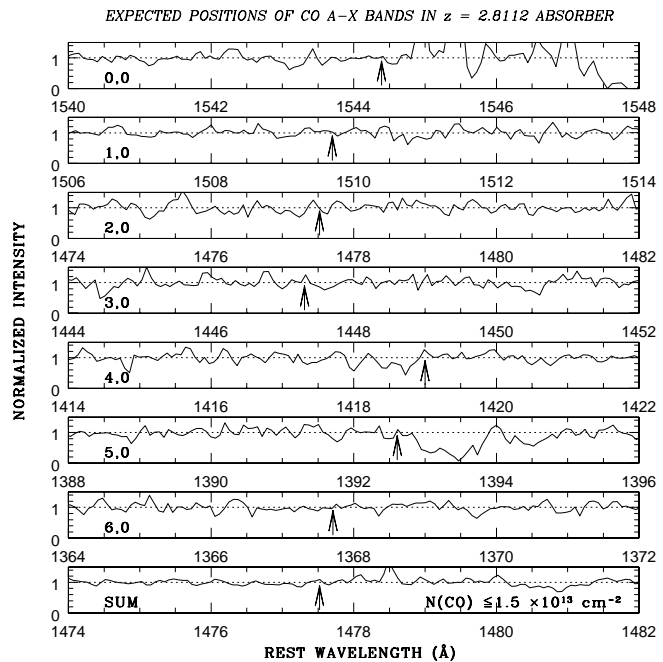


Fig. 3. Plot showing the spectrum in the rest wavelength of different A-X bands in CO due the $z_{\text{abs}} = 2.8112$ damped system. The centres of each band is marked with an arrow.

In order to improve the signal to noise we followed the stacking method prescribed by Levshakov et al. (1989). The resulting combined spectrum at the rest frame of the 2-0 band is given in the last panel of the Fig. 3. No clear line is seen at the expected position. Using the weighted oscillator strength of all the bands and a velocity dispersion of 9 km s^{-1} , similar to H_2 , we obtain a 3σ upper limit for the column density of $N(\text{CO}) \simeq 1.5 \times 10^{13} \text{ cm}^{-2}$. This limit is consistent with other determinations (Ge et al. 1997). This is a factor of two higher than the upper limits obtained for the damped systems along the line of sight to PHL 957 and 1331+170 (Levshakov et al. 1989). This limit leads to $N(\text{CO})/N(\text{H}) \leq 7 \times 10^{-9}$.

Federman et al. (1980) have estimated the CO column density along the lines of sight towards 48 bright stars. The results of their analysis suggest that CO is readily detected when $N(\text{H}_2) > 10^{19} \text{ cm}^{-2}$. Thus the non detection of CO in the $z = 2.8112$ system is consistent with

the $N(\text{CO})/N(\text{H}_2)$ ratios seen in the diffuse interstellar medium. They also noted that $N(\text{C I})$ is, on average, 10 times larger than $N(\text{CO})$. If $N(\text{C I})$ is greater than $N(\text{CO})$ in the system under consideration also, then the upper limit on $N(\text{C I})$ suggests that the value of $N(\text{CO})$ should be an order of magnitude less than the derived upper limit.

4. The low $N(\text{C I})/N(\text{H}_2)$ ratio

The ratios $N(\text{C I})/N(\text{H I}) < 2.2 \cdot 10^{-9}$ and $N(\text{H}_2)/N(\text{H I}) = 2.7 \cdot 10^{-5}$ derived from this study are surprisingly low. Indeed in the interstellar medium of our Galaxy, all the clouds with $\log N(\text{H I}) > 21$ have $\log N(\text{H}_2) > 19$ and $\log N(\text{C I}) > 14$ (Jenkins & Shaya 1979). It thus may be interesting to investigate the reasons for such low ratios.

Formation of H_2 is expected on the surface of dust grains if the gas is cool, dense and mostly neutral, and from the formation of negative hydrogen if the gas is warm and dust free (see e.g. Jenkins & Peimbert 1997). Given the neutral hydrogen column density of this system and the evidence for depletion onto dust grains (see however Warren & Møller 1996), the first process should dominate. Destruction is mainly due to UV photons. The effective photodissociation of H_2 takes place in the energy range 11.1–13.6 eV, through Lyman-Werner band line absorption. Since the ionization potential of C I is 11.2 eV, it is sensitive to the same photo-ionization field as H_2 in the neutral phase. If the H_2 lines are saturated then the cloud is self-shielded against further photodissociation of H_2 . In this case however large values of $N(\text{H}_2)$ to $N(\text{C I})$ ratio are easily produced.

We run grids of photoionization models using CLOUDY (Ferland 1993). These models take into account photo-dissociation of H_2 molecules using the approximations outlined by Tielens and Hollenbach (1985). The incident radiation field is averaged over the wavelength interval 912–1109 Å and is redistributed according to the interstellar radiation spectrum given by Habing (1968).

In our calculations we take the gas phase abundances to be 1/10 of solar. The grain composition is assumed to be similar to that of the Galactic ISM and we use the dust to gas ratio as a free parameter. We perform the photoionization calculations for different ionizing radiation spectra and a range of ionizing parameters, U . We consider four possible spectral energy distribution for the incident radiation field which are (1) a simple power-law of index α , $F(\nu) \propto \nu^{-\alpha}$; (2) a power-law with a "big bump" modeled as a black-body of temperature 50 000 K, the relative contributions of the power-law spectrum and the black-body is characterized by the index $\alpha_{\text{ox}} = \log F(2500 \text{ \AA})/F(2 \text{ keV})$; (3) a typical spectrum of AGNs (Mathews & Ferland 1987); and (4) a starburst (Charlot, private communication). The optical to X-ray spectral energy distribution of PKS 0528–250 is not well defined. Wilkes et al. (1994) failed to detect X-ray emission from this quasar in their Einstein IPC data. They

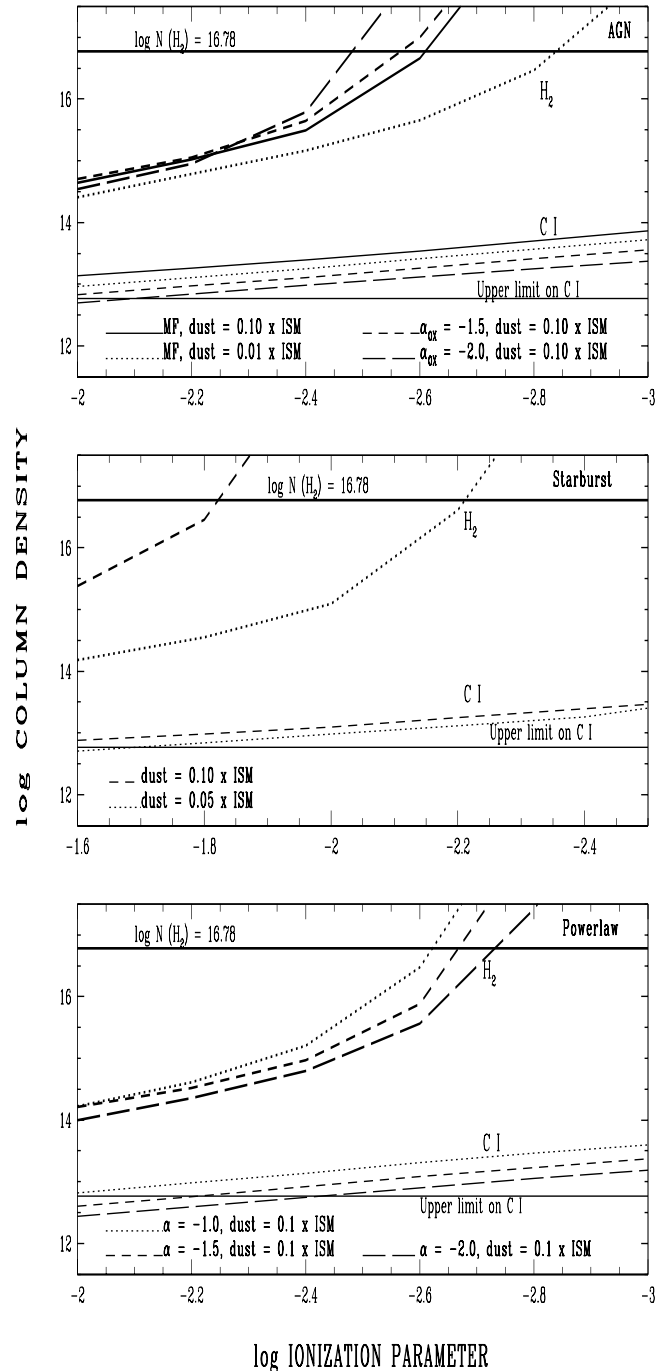


Fig. 4. H_2 and C I column densities versus ionization parameter for different ionizing spectra (the SEDs are given in Fig. 5). The cloud is modeled as a slab of constant density $n = 100 \text{ cm}^{-3}$ illuminated on one side by an incident flux, resulting in an ionization parameter U (ratio of the density of ionizing photons to the density of hydrogen). Metallicity is a tenth of solar and the amount of dust is taken as a fraction of the ISM dust content.

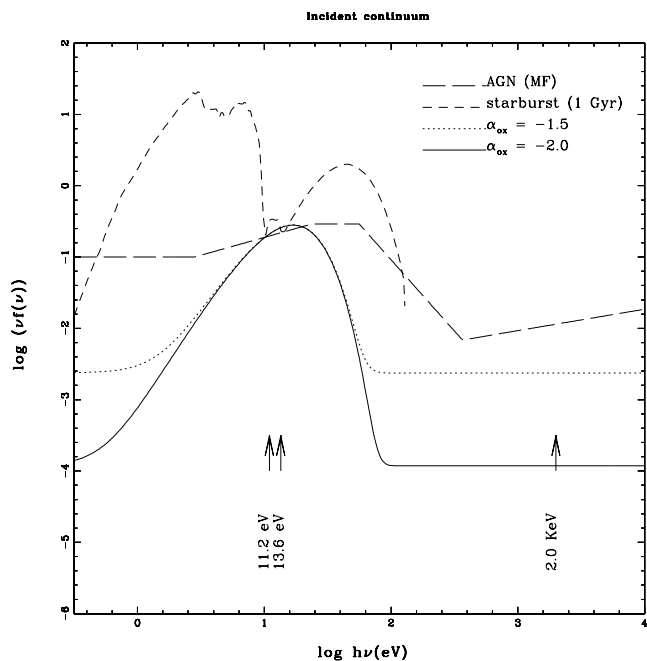


Fig. 5. Spectral energy distributions of the incident flux irradiating the cloud from the models presented in the text. The small-dashed curve corresponds to a 1 Gyr old starburst; the long-dashed curve is the AGN spectrum described by Mathews & Ferland (1987); the solid and dotted lines correspond to power-law spectra with UV big-bumps, modeled as a black-body of temperature 50 000 K.

derive an upper limit on α_{ox} of -1.34 . It is known that a typical quasar will have α_{ox} in the range -1.0 to -2.0 with a mean of -1.5 (e.g. Wilkes et al. 1994). Thus in our model we use either $\alpha_{\text{ox}} = -1.5$ or -2.0 .

The predicted column densities of H_2 and C I as a function of the ionizing parameter U for different models are given in Fig. 4 (the SEDs are shown for direct comparison in Fig. 5). For all models, $\log N(\text{H I}) = 21.35$ and $n_{\text{H}} = 100 \text{ cm}^{-3}$. We have checked that the exact value of n_{H} has little effect on the results.

To reproduce the small $N(\text{C I})/N(\text{H I})$ ratio, the spectrum must be steep to favor ionization of C I . This is why a power-law spectrum with $\alpha = -2$, a "big-bump" spectrum with $\alpha_{\text{ox}} = -2$ and the starburst spectrum can reproduce the ratio with somewhat different ionizing parameters. The "big-bump" spectrum is favored because the X-ray tail maintains the temperature of the neutral gas above 100 K. The other models imply too low a temperature compared to what we derived from the H_2 features. However all the models fail to reproduce at the same time the H_2 column density. It is apparent from the figure that steeper spectra could meet the constraints. However again the temperature would be too low. Moreover, all the models predict $\log N(\text{Mg I}) > 13.5$. This is a factor of seven larger than the upper limit we derived from the Lu

et al. (1996) data. In the framework of these models, the only solution we can find is to decrease the abundances of carbon by a factor of two and that of magnesium by a factor of seven. This could reflect true relative abundances or depletion onto dust grains.

Dust is needed to explain the H_2 column density as is apparent from Fig. 4. The H^- process is more efficient than the dust process at temperature $T > 500 \text{ K}$ and when n_e is not negligible, thus in the partially ionized region. However the very large H I column density of this damped $\text{Ly}\alpha$ system requires most of the gas to be neutral where this process is negligible because of the low temperature resulting from the steep spectrum needed to explain the lack of C I and Mg I .

5. Conclusion

By fitting the different H_2 transitions that we detect in a high resolution spectrum of PKS 0528–250, we derive $\log N(\text{H}_2) \sim 16.78$ and $T_{\text{ex}} \sim 200 \text{ K}$ that is most certainly the true kinetic temperature of the gas. For this temperature, the relative populations of rotational levels 0 to 4 indicate that the density is of the order of 1000 cm^{-3} . Therefore the dimension of the neutral cloud along the line of sight is less than 1 pc. It must be noticed that the damped absorber must cover the broad line region. Indeed there is no residual flux in the bottom of the $\text{Ly}\alpha$ absorption line which completely absorbs the $\text{Ly}\alpha$ emission from the quasar over more than 5000 km s^{-1} (Møller & Warren 1993). Since the dimension of the BLR in QSOs can be approximated as $R \sim 0.3 L_{46}^{0.5}$ where L_{46} is the bolometric luminosity in units of $10^{46} \text{ erg s}^{-1}$ (Collin, private communication). The radius of the BLR in PKS 0528–250 is thus of the order of 10 pc. The transverse dimension of the damped cloud must be thus larger than 10 pc and the cloud must be quite flat.

We can derive an upper limit on the transverse dimension of the cloud by interpreting the non-detection of redshifted 21 cm absorption (Carilli et al. 1996) as an effect of partial covering factor of the continuum radio emission by the cloud. Indeed the size of the radio source is 1 arcsec or $5h_{75}^{-1} \text{ kpc}$. If the spin temperature is equal to the kinetic temperature we derived in sect. 3.2, this implies that the covering factor should be less than 0.3 and thus the radius of the cloud along the transverse direction is less than 1 kpc.

We determine upper limits for the C I , Mg I and CO column densities ($\log N(\text{C I}) < 12.7$, $\log N(\text{Mg I}) < 12.8$ and $\log N(\text{CO}) < 13.2$). Based on simple photoionization models we conclude that (i) no simple model can reproduce at the same time the low $N(\text{C I})/N(\text{H I})$, $N(\text{Mg I})/N(\text{H I})$ ratios and the presence of molecules at the level observed; (ii) steep spectra are required to reproduce the low $N(\text{C I})/N(\text{H I})$ and $N(\text{Mg I})/N(\text{H I})$ ratios but they predict temperatures smaller than 100 K in conflict with the excitation temperature derived from the

H₂ transitions; (iii) the only way to keep the temperature as high as 200 K is to allow for some X-ray flux heating the gas; (iv) in the framework of these models, dust is needed to produce the observed amount of molecules; (v) the gas phase abundances of carbon and especially magnesium should be smaller than 0.1 of solar.

In view of the models we explored, the most likely ionizing spectrum is a composite of a UV-”big bump” possibly produced by a local starburst and a power-law spectrum from the QSO that provides the X-rays.

Acknowledgements. We thank Drs. L. Cowie and J. Bechtold for useful information, Stéphane Charlot for providing us with the new models of starburst SED and an anonymous referee for insightful comments.

References

- Barvainis R., et al., 1994, *Nature* 371, 586
 Bergeron J., Boissé P., 1991, *A&A* 243, 344
 Black J.H., Dalgarno, A., 1973, *ApJL* 184, L101
 Black J.H., Chaffee F.H., Foltz C.B., 1987, *ApJ* 317, 442
 Carilli C.L., Lane W., de Bruyn A.G., Braun R., Miley G.K., 1996, *AJ* 111, 1830
 Chaffee F.H., Black J.H., Foltz C.B., 1988, *ApJ* 335, 584
 Federman S.R., Glassgold A.E., Jenkins E.B., Shaya E.J., 1980, *ApJ* 242, 545.
 Ferland G.J., 1993, Univ. of Kentucky, Depart. of Physics and Astronomy Internal Report
 Foltz C.B., Chaffee F.H.Jr., Black J.N., 1988, *ApJ* 324, 267
 François P., 1987, *A&A* 176, 294
 Ge J., Bechtold J., 1997, *ApJ*, 477, L73
 Ge J., Bechtold J., Walker C., Black J.H., 1997, *ApJ* 486, 727
 Gratton R.G., Sneden C., 1991, *A&A* 241, 501
 Guilloteau S., Omont A., McMahon R., Cox P., Petitjean P., *A&A* 328, L1
 Habing H. J., 1968, *Bull. Astr. Inst. Netherlands* 19, 421.
 Haehnelt M.G., Steinmetz M., Rauch M., 1997, *astro-ph/9706201*
 Jenkins E.B., Peimbert A., 1997, *ApJ* 477, 265
 Jenkins E.B., Shaya E.J., 1979, *ApJ* 231, 55
 Jura M., 1974, *ApJ* 191, 375
 Jura M., 1975, *ApJ* 197, 581
 Khare P., Srianand R., York D.G., et al., 1997, *MNRAS* 285, 167
 Le Brun V., Bergeron J., Boissé P., Deharveng J.M., 1996, *A&A* (submitted)
 Ledoux C., Petitjean P., Bergeron J., Wampler J., Srianand R., 1998, *A&A* in press
 Levshakov S.A., Chaffee F.H., Foltz C.B., Black J.H., 1992, *A&A* 262, 385.
 Levshakov S.A., Foltz C.B., Chaffee F.H., Black J.H., 1989, *AJ* 98, 2052.
 Levshakov S.A., Varshalovich D.A., 1985, *MNRAS* 212, 517
 Lu L., Sargent W.L.W., Barlow T.A., Churchill C.W., Vogt S.S., 1996, *ApJS* 107, 475
 Magain P., 1989, *A&A* 209, 211
 Mathews W.G., Ferland G., 1987, *ApJ* 323, 456
 Meyer D.M., Welty D.E., York D.G., 1989, *ApJL* 343, L37
 Meyer D.M., York D.G., 1987, *ApJL* 319, L45
 Møller P., Warren S.J., 1993, *A&A* 270, 43
 Morton D.C., 1991, *ApJS* 77, 119
 Morton D.C., Dinerstein H.L., 1976, *ApJ* 204, 1
 Nishimura S., 1968, *Annals of the Tokyo Astronomical Observatory, Ser 2*, 11, 33
 Ohta K., Yamada T., Nakanishi K., Kohno K., Akiyama M., Kawabe R., 1996, *Nature* 382, 426
 Omont A., Petitjean P., Guilloteau S., McMahon R., Solomon P.M., 1996, *Nature* 382, 428
 Petitjean P., Bergeron J., 1994, *A&A* 283, 759
 Pettini M., King D.L., Smith L.J., Hunstead R.W., 1996, *astro-ph/9607093*
 Pettini M., Smith L.J., Hunstead R.W., King D.L., 1994, *ApJ* 426, 79
 Pettini M., Smith L.J., King D.L., Hunstead R.W., 1997, *astro-ph/9704102*
 Prochaska J.X., Wolfe A.M., 1997, *astro-ph/9704169*
 Roth K.C., Blades J.C. 1995, *ApJ* 445, L95
 Savage B.D. Sembach K.R., 1996, *ARA&A* 34, 279
 Sneden C., Crocker D.A., 1988, *ApJ* 335, 406
 Songaila A., Cowie L.L., 1995, *AJ* (submitted)
 Tielens A.G.G.M., Hollenbach D., 1985, *ApJ* 291, 722
 Warren S.J., Møller P., 1996, *A&A* 311, 25
 Wilkes B.J., Tananbaum H., Worrall D.M., Avni Y., Oey M.S., Flanagan J., 1994, *ApJS* 92, 53
 Wiklind T., Combes F., 1994, *A&A* 288, 41
 Wolfe A.M., 1996, in ‘QSO absorption lines’, G. Meylan (Ed.), Springer, Garching, p.13

This article was processed by the author using Springer-Verlag L^AT_EX A&A style file L-AA version 3.